*Biochimica et Biophysica Acta*, 394 (1975) 633–645


BBA 76998

# THE STRUCTURE AND THERMOTROPISM OF THYMOCYTE PLASMA MEMBRANES AS REVEALED BY LASER-RAMAN SPECTROSCOPY

SURENDRA P. VERMA, DONALD F. H. WALLACH and RUPERT SCHMIDT-ULLRICH

*Division of Radiobiology, Therapeutic Radiology Department, New England Medical Center Hospital, 171 Harrison Avenue, Boston, Mass. 02111 (U.S.A.)*

(Received December 30th, 1974)

## SUMMARY

1. Plasma membranes from rabbit thymocytes have been analyzed by laser-Raman spectroscopy over the 800–3000 $cm^{-1}$ region and the spectra compared with those of endoplasmic reticulum, as well as relevant liposome systems.

2. Evaluation of the Amide I and Amide III regions indicates that thymocyte plasma membranes, but not endoplasmic reticulum, contain appreciable $\beta$-structure peptide. This conclusion is supported by infrared spectroscopy.

3. Evaluation of the 2890 $cm^{-1}$ : 2850 $cm^{-1}$ intensity ratio of plasma membranes as a function of temperature, using an integration technique, demonstrates a thermotropic lipid transition centered near 23 °C. This transition is less sharp than one observed with egg lecithin in this temperature range.

4. The significance of the thermotropic transition is evaluated in view of the lack of thermotropic lipid-protein segregation detectable by freeze-fracture electron microscopy (Wunderlich, F., Wallach, D. F. H., Speth, V. and Fischer, H. (1973) Biochim. Biophys. Acta 373, 34–43).

## INTRODUCTION

During our explorations into the structure and function of lymphocyte membranes, we discovered that the nuclear membranes of these cells can undergo a reversible, thermotropic segregation of their lipid and protein moieties [1]. This segregation manifests itself on freeze-fracture electron micrographs in the altered concentration and topology of intramembranous particles observed after cells are cooled below 22 °C.

This thermotropic segregation of lipid from protein is not observed in the plasma membranes of lymphoid cells [1], a fact which might be attributed to the high cholesterol: phospholipid ratio of these membranes, a restricted protein mobility, or both. We have, accordingly, subjected thymocyte plasma membranes,

Abbreviation: HEPES, 4-(hydroxymethyl)-1-piperazinylethane-2-sulfate.

isolated by methods [2] designed for metabolic experimentation [3, 4], to structural analysis by laser-Raman spectroscopy [5]. As we have recently shown for erythrocyte ghosts [6], biomembranes can yield well resolved Raman spectra which inform about the structure of membrane proteins and lipids as well as the interaction of these moieties.

In this initial report on the analysis of lymphocyte membranes by laser-Raman spectroscopy, we focus on the plasma membranes of rabbit thymocytes, but include pertinent data on endoplasmic reticulum and model systems. We demonstrate that the plasma membrane lipids do undergo a thermotropic structure transition, but that this is poorly cooperative. We further show that thymocyte plasma membranes contain appreciable $\beta$-structure peptide and that endoplasmic reticulum, but not plasma membrane, contains conjugated polyenes that are probable protein bound.

## EXPERIMENTAL

*Preparation of thymocyte membranes.* Microsomal membranes were prepared from freshly isolated rabbit thymocytes as in ref. 2. Washed cells were resuspended at a concentration of $5 \cdot 10^7$ cells/ml in 0.075 M KCl, 0.065 M NaCl, 0.25 mM $MgCl_2$, 0.01 M 4-(hydroxymethyl)-1-piperazinylethane-2-sulfate (HEPES) pH 7.5, and disrupted by nitrogen cavitation. We sedimented nuclei, mitochondria and lysosomes at $6 \cdot 10^5$ $g \cdot$ min (Beckman centrifuge J 21) and pelleted the small particle fraction at $10^7$ $g \cdot$ min (Beckman Spinco ultracentrifuge L2 65, Rotor 60 Ti). We then washed the microsomes, first with 0.01 M HEPES, pH 7.5, and then with 0.001 M HEPES, pH 7.5 ($10^7$ $g \cdot$ min) to eliminate trapped cytoplasmic proteins and to dissociate membrane-bound ribosomes. After the last washing, microsomes were resuspended in 0.001 M HEPES, 0.001 M $MgCl_2$, pH 8.2, applied to a dextran gradient (Dextran T-150, Pharmacia, Sweden) (maximum density 1.09) as in ref. 2 and centrifuged for $10^8$ $g \cdot$ min (Beckman Spinco L2 65, Rotor SW 56). The two membrane fractions obtained, plasma membranes and endoplasmic reticulum [2] were collected from the gradient and washed twice in 0.005 M phosphate, pH 8.0, by pelleting them at $1.2 \cdot 10^7$ $g \cdot$ min.

Chemical analyses [2] reveal phospholipid/protein ratios of 822 and 272 nmol/mg protein for plasma membranes and endoplasmic reticulum, respectively. The RNA contents of the plasma membrane and endoplasmic reticulum fractions were 0.5 and about 5 %, respectively. The plasma membranes exhibit a cholesterol/phospholipid molar ratio of approx. 1.2.

*Chemicals.* Egg lecithin (unsaturated) was obtained from Lipid Products (South Nutfield, Great Britain), dipalmitoyl lecithin, dipalmitoyl phosphatidylethanolamine and sphingomyelin from Serdary Research Laboratories (London, Ontario, Canada), cholesterol from Sigma (St. Louis, Mo., U.S.A.) and melittin from Nutritional Biochemicals (Cleveland, Ohio, U.S.A.). AgCl plates for infrared measurements were purchased from Harshaw (Solon, Ohio, U.S.A.). All other reagents were of analytical grade.

*Preparation of liposomes.* Phosphatide liposomes were prepared as described previously [7]. The phosphatide concentration used were of the order of 0.12 M.

*Infrared spectra.* Infrared spectra were recorded on air-dried membrane films [8] using a Perkin-Elmer infrared spectrophotometer.

*Raman spectroscopy.* Membrane vesicles and liposomes with and without melittin were transferred to 0.9–1 mm internal diameter Kimex Capillaries. After sealing, the sample capillaries were placed in a Harney-Miller Cell [9] for temperature control. The temperature was regulated by a flow of nitrogen regulated by a telethermometer. Temperature control was checked by melting point measurements on standard lipids in the laser beam.

Raman spectra were recorded by a Ramalog 4 Raman spectrometer (Spex Industries, Metuchen, N. J., U.S.A.) interfaced to an Interdata (Model 70) computer. An $Ar^+$ laser (Spectra Physics model 164), tuned at 488 nm or 514.5 nm, 300 mW power at the sample, was used as an excitation source. The Raman scattering at right angles to the laser beam was detected by a thermo-electrically cooled photomultiplier (RCA 31034) and was recorded in terms of photons/s. The "dark" counts of the photo cell were < 100 counts/s. Raman scattering from the sample gave counts in the order of $10^3$–$10^4$/s. Scanning was done through the computer (loaded with the VIE8D Ramancomp Computer Program, Spex Industries). We used the following specifications for scanning. Maximum time and minimum time at each data point were 3 and 1 s, respectively; photon counts, $10^4$/s maximum, 100/s minimum; scanning step, one wave number. The program does not scan the spectrometer at a rate linear with respect to time. Rather, scans are incremental between data points and no counts are recorded when the spectrometer is moving between data points. The photon counts were stored in the computer memory during scanning (2–4 scans). The averaged, stored spectra were then plotted on the Ramalog recorder.

## RESULTS AND DISCUSSION

### *2800–3000 $cm^{-1}$*

Fig. 1 depicts the Raman scattering by thymocyte plasma membranes and endoplasmic reticulum in the 2800–3000 $cm^{-1}$ region. The C-H stretching vibrations of both membrane proteins and membrane lipids appear in this frequency range. We observe scattering peaks near 2850, 2890, 2910 and 2940 $cm^{-1}$ and shoulders at 2870 and 2960 $cm^{-1}$. The C-H stretching modes are strong and vary little in frequency (unlike, for example, O-H or amide vibrations): they can therefore be rather easily assigned.

The 2850 $cm^{-1}$ band has been previously assigned to symmetric $CH_2$ stretching vibrations of phosphatides [10]. Concordantly, lipids such as phosphatidylethanolamine (Fig. 1), lecithin [6], fatty acids [11] and sphingomyelin (Table I) show a strong, sharp band at 2850 $cm^{-1}$. However, $CH_2$-containing amino acids, polypeptides and proteins do not exhibit Raman scattering at this frequency [12], even though amino acids such as lysine and arginine have substantial $CH_2$ sequences. It appears, therefore, that the 2850 $cm^{-1}$ band of the membranes is due to the acyl chains of membrane lipids.

The 2870 $cm^{-1}$ shoulder and 2907 $cm^{-1}$ band are not observed with liposomes (Fig. 1) or with solutions of phosphatides in organic solvents, but a band at 2865 $cm^{-1}$ has been reported for long chain hydrocarbons with triclinic chain packing [11]. However, we and others have observed Raman scattering near 2875 $cm^{-1}$ with a variety of amino acids, polypeptides and proteins. Examples are 2870 $cm^{-1}$ for bovine serum albumin [6], 2870 $cm^{-1}$ for thymidylate synthetase (our unpublished

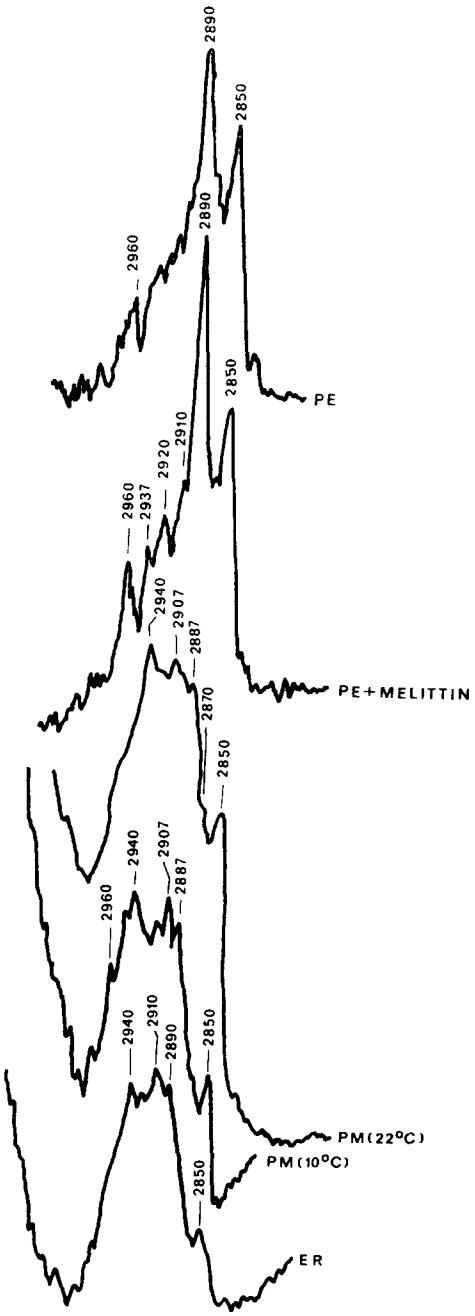


Fig. 1. Raman spectra in the 2900 $cm^{-1}$ region of thymocyte plasma membrane (PM) and endoplasmic reticulum (ER), dipalmitoyl phosphatidylethanolamine (PE) with and without melittin. Excitation wavelength 488 nm. Resolution about 5 $cm^{-1}$; power 300 mW. The Raman spectra of phosphatidylethanolamine with and without melittin and endoplasmic reticulum were recorded at $18 \pm 2$ °C.

TABLE I

RAMAN FREQUENCIES FOR THYMOCYTE PLASMA MEMBRANE, ENDOPLASMIC RETICULUM MEMBRANES AND SPHINGOMYELIN

Sh, shoulder; $\nu$, stretching; $\delta$, deformation.

| Plasma membrane ($cm^{-1}$) | Endoplasmic reticulum ($cm^{-1}$) | Sphingomyelin ($cm^{-1}$) | Tentative assignment |
|---|---|---|---|
| 2960 | – | 2960 (Sh) | asymmetrical $\nu$ $CH_3$ |
| 2940 | 2940 | 2940 | asymmetrical $\nu$ $CH_2$ |
| 2907 | 2910 | – | $\nu$ $CH_2$ |
| 2887 | 2890 | 2890 | symmetrical $\nu$ ($CH_2$ and $CH_3$) |
| 2870 | – | – | symmetrical $\nu$ ($CH_2$ and $CH_3$) |
| 2850 | 2850 | 2850 | symmetrical $\nu$ $CH_2$ |
| 1660 | 1670 | 1677 | Amide I + water |
| 1640 | – | 1663 | |
| – | 1610 | 1645 | Trp |
| – | 1528 | | (–C=C–) conjugated |
| 1460 | 1470 | 1460 | $\delta$ ($CH_2$ and $CH_3$) |
| 1440 | 1450 | 1440 | |
| 1432 | – | – | |
| 1375 | 1370 | – | Trp |
| 1340 | 1340 | – | $\delta$ CH |
| 1300 | – | 1300 | rocking $CH_2$ |
| 1267 | 1270 | – | |
| 1240 (Sh) | – | – | Amide III |
| 1228 | – | – | |
| 1200 | – | – | |
| – | 1155 | – | $\nu$ (=C–C=) in conjugated |
| 1150 | – | – | $\nu$ (–C–C) + (C–N) |
| 1130 | 1130 | 1130 | |
| 1100 | 1097 | – | Phosphate |
| 1080 | 1080 | 1092 | |
| 1062 | – | 1065 | $\nu$ (C–C) + (C–N) |
| 1015 | – | – | Trp + Phe |
| 1003 | 1005 | | |
| 960 | 970 | 960 | $\nu$ (C–C) |
| 922 | 920 | 925 | |
| 860 | 855 | – | Ty |

results), 2876 $cm^{-1}$ for poly-L-lysine [13] and 2872 $cm^{-1}$ for solid chymotrypsinogen [12]. We therefore assign the shoulder near 2870 $cm^{-1}$ to hydrocarbon residues in the amino acid side chains of membrane proteins. The band near 2910 $cm^{-1}$ can be similarly assigned [12].

Thymocyte plasma membranes and endoplasmic reticulum show strong Raman scattering at 2887 and 2890 $cm^{-1}$, respectively (Fig. 1). Long-chain lipids also show a strong band at 2890 $cm^{-1}$ and this has been previously assigned to overlapping $CH_2$ and $CH_3$ (symmetrical) vibrations [10]. However, proteins, polypeptides and amino acids yield no scattering at 2890 $cm^{-1}$.

The maximum number of $CH_2$ groups, in amino acid side chains (four) occurs in lysine, yet lysine or poly-L-lysine shows no 2890 $cm^{-1}$ band; nor do short-chain

alkanes [14]. We therefore propose that the 2890 $cm^{-1}$ band arises from lipid acyl-chain segments of length greater than four $CH_2$ residues and from $CH_3$.

The band at 2940 $cm^{-1}$ includes contributions from both membrane proteins and lipids. Dipalmitoyl lecithin exhibits only a weak shoulder near 2935 $cm^{-1}$ [10] but egg lecithin has a distinct band at this frequency and the intensity of this band increases with prolonged sonication. Proteins and polypeptides show strong scattering in this region, e.g. 2926, 2940, 2951, 2936 and 2923 $cm^{-1}$ for chymotrypsinogen [12], bovine serum albumin [6], ribonuclease [12], poly-L-lysine [13] and poly-L-glutamate [12], respectively. We suggest that the membrane scattering bands near 2940 $cm^{-1}$ arise from asymmetrical [12] $CH_2$ vibrations in short hydrocarbon segments. The lipid contribution would then be from $CH_2$ residues separated by C = C bonds in the unsaturated chain of phosphatides, whereas the protein contribution would be from the $CH_2$-containing amino acids. The latter contribute the bulk of membrane $CH_2$ residues and we conclude that the band near 2940 $cm^{-1}$ arises predominantly from membrane proteins.

*The 2910 $cm^{-1}$ : 2850 $cm^{-1}$ intensity ratio**

Since the $\approx$ 2910 $cm^{-1}$ band arises from membrane protein and the 2850 $cm^{-1}$ band from lipids, the relative integrated intensities of these bands should reflect the protein : lipid ratio. We observed a ratio of 1.4 for plasma membrane and 4.0 for endoplasmic reticulum, suggesting that these membranes contain 58 and 80 % protein, respectively. These values are consistent with biochemical analyses [2].

*Chain Mobility*

As we will detail further on, in phosphatide liposomes, the integrated 2890 $cm^{-1}$ : 2850 $cm^{-1}$ scattering ratio decreases with increasing temperature (Fig. 2):

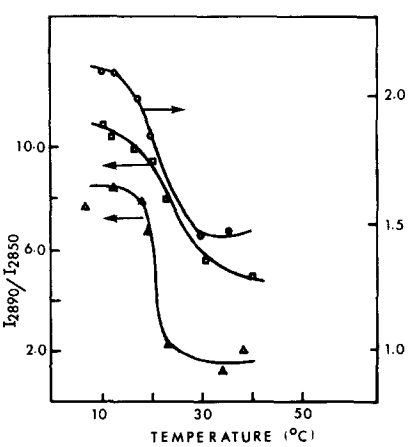


Fig. 2. The plot of ratio of integrals between 2860–2900 ($I_{2890}$) and 2830–2860 $cm^{-1}$ ($I_{2850}$) vs temperature. In the case of plasma membranes $I_{2890}$ represents the integral between 2875 and 2895 $cm^{-1}$ (see text for details). The points marked in the curves are an average value of four different recordings at a particular temperature. ○, plasma membrane; □, egg lecithin + cholesterol; △, egg lecithin.

* 2910 $cm^{-1}$ : 2850 $cm^{-1}$ in endoplasmic reticulum; 2907 $cm^{-1}$ : 2850 $cm^{-1}$ in plasma membrane.

this trend shows a discontinuity centered near 20 °C. Below this temperature, the ratio changes by 0.04/°C. In view of these facts, one might expect that, in a given system, the 2890 $cm^{-1}$ : 2850 $cm^{-1}$ intensity ratio will reflect acyl chain mobility as a function of lipid protein interaction at a given temperature. We have evaluated this possibility for the interaction of phosphatidylcholine and phosphatidylethanolamine with melittin, an amphipathic polypeptide known to restrain phosphatide acyl chain motion [15].

The intensity ratios (2890 $cm^{-1}$ : 2850 $cm^{-1}$) of dipalmitoyl lecithin and dipalmitoyl phosphatidylethanolamine were 1.20 and 1.29, respectively. Addition of melittin ($10^{-3}$ M) to the phosphatides (0.12 M) altered the 2800–3000 $cm^{-1}$ region of the spectra (Fig. 1) and increased the ratios to 1.36 and 1.54, respectively. We interpret these changes to reflect the restriction on acyl chain mobility induced by melittin. The greater effect with phosphatidylethanolamine is compatible with the greater interaction between this phosphatide and melittin. The intensification of the bands at 2910, 2920 and 2937 $cm^{-1}$ (Fig. 1) may reflect immobilization of the $-CH_2-CH_2-$ moiety of phosphatidylethanolamine due to ionic bonding [15] between the anionic lipid and the basic polypeptide. At the concentrations used, melittin itself does not contribute significant scattering.

Turning to the membranes (Fig. 1), we find that the 2890 $cm^{-1}$ : 2850 $cm^{-1}$ intensity ratio (integrated) is 1.3 in plasma membrane and 4.0 in endoplasmic retic-

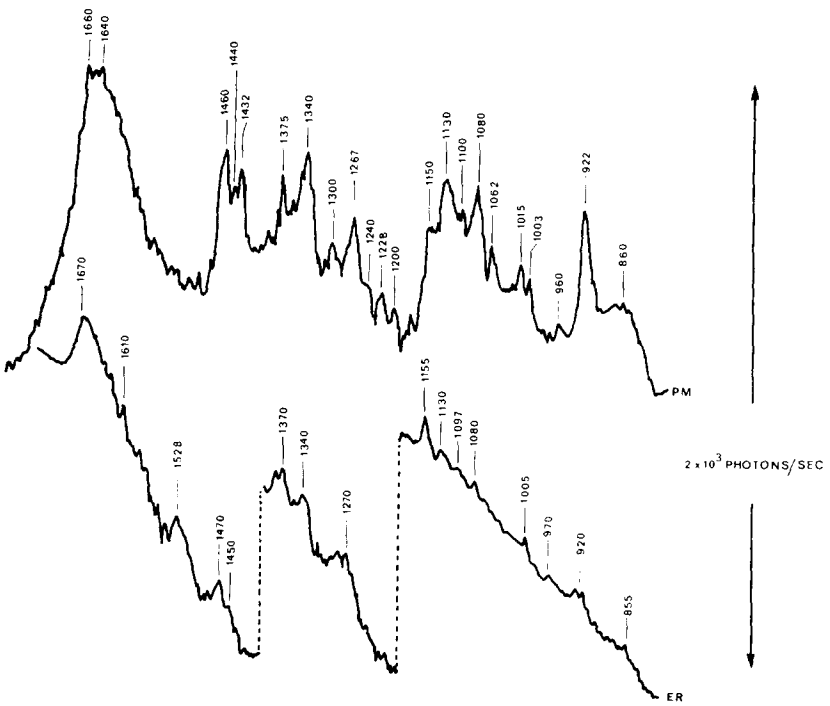


Fig. 3. Raman spectra in the 800–1800 $cm^{-1}$ region of thymocyte plasma membrane (PM) and endoplasmic reticulum (ER). Excitation wavelength 488 nm; power 300 mW; resolution about 5 $cm^{-1}$; temperature 18±2 °C. Raman intensities are in photons/s (Scale marked). Dotted vertical lines in the endoplasmic reticulum spectrum indicate changes in the background suppression.

ulum, almost indentical to the protein : lipid ratios. The different 2890 $cm^{-1}$ : 2850 $cm^{-1}$ intensity ratios of the two membranes may arise in part to overlap between the 2890 and 2910 $cm^{-1}$ bands and may in part be due to a greater degree of apolar lipid-protein interaction than exist in plasma membranes. We also cannot fully exclude a contribution due to the different cholesterol : phospholipid ratios of the two membranes. However, as shown below and in Fig. 2, the effects of cholesterol on the intensity ratio 2890 $cm^{-1}$ : 2850 $cm^{-1}$ are numerically much smaller than what we describe here. The smaller ratio, 1.54, observed in the melittin-phosphatidylethanolamine system can be attributed to the low protein : lipid weight ratio, 0.03, employed to avoid interference by melittin scattering.

*Amide I region: 1630–1670 $cm^{-1}$*

As shown in Fig. 3, plasma membrane vesicles exhibit two peaks in this region, at 1640 $cm^{-1}$ and at 1660 $cm^{-1}$: a small shoulder is observed at 1670 $cm^{-1}$. Fig. 4, an expanded scale spectrum of the Amide I region after subtraction of the scattering contribution of water (centered at 1640 $cm^{-1}$), reveals that the 1660 $cm^{-1}$ band is predominant. In contrast, endoplasmic reticulum yields a single peak at 1670 $cm^{-1}$.

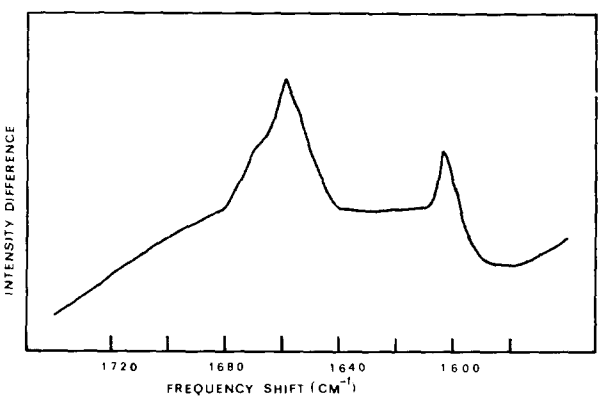


Fig. 4. Difference Raman spectrum in the thymocyte plasma membrane in the Amide I region. The integrated water spectrum computed for 5 $cm^{-1}$ intervals is subtracted from the integrated membrane spectrum.

Raman scattering in the Amide I region should in principle provide information about the average secondary structure of membrane proteins. Thus, $\alpha$-helical homopolypeptides exhibit a strong line near 1650 $cm^{-1}$, e.g. 1654 $cm^{-1}$ for poly-L-alanine [16], 1652 $cm^{-1}$ for poly-benzyl-L-glutamate [17], 1652 $cm^{-1}$ for poly-L-leucine and 1645–1652 $cm^{-1}$ for poly-L-lysine [17, 13, 18]. The major Amide I bands of $\beta$-structured homopolypeptides, in contrast, lie between 1663 and 1764 $cm^{-1}$, e.g. 1663 $cm^{-1}$ for poly-L-alanine [12], 1666 $cm^{-1}$ for poly-L-valine [12], 1668–1672 $cm^{-1}$ for poly-L-serine [17] and 1670–1672 $cm^{-1}$ for poly-L-lysine [13, 18]. Homopolypeptides in the unordered state do not yield sharp Raman peaks: broad bands have been reported at 1649 $cm^{-1}$ for poly-L-glutamate [12] and 1657 $cm^{-1}$ for poly-L-lysine [13].

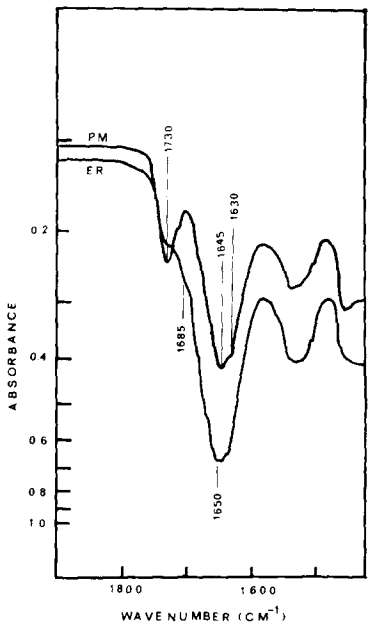


Fig. 5. Infrared absorption spectra (Amide I region) of thymocyte plasma membrane (PM) and endoplasmic reticulum (ER) deposited on AgCl plates. The frequencies at top are for plasma membrane; those at the bottom are for endoplasmic reticulum.

According to the Raman data on homopolypeptides, the 1660 $cm^{-1}$ band in plasma membranes suggests a substantial proportion of peptide in the $\beta$-conformation. Our infrared spectra (Fig. 5) support this conclusion. The plasma membrane fragments show a broad maximum at 1650–1645 $cm^{-1}$ with a small shoulder near 1635 $cm^{-1}$, whereas endoplasmic reticulum yields a sharper peak, maximal at 1650 $cm^{-1}$. $\alpha$-Helical and unordered homopolypeptides exhibit maximal Amide I absorption at 1652 and 1656 $cm^{-1}$ whereas the Amide I peak of $\beta$-structured polypeptides lies near 1630 $cm^{-1}$. According to these criteria, endoplasmic reticulum membrane proteins are in helical and/or unordered array, but plasma membranes contain appreciable proportions of $\beta$-structure.

*Amide III region: 1200–1300 $cm^{-1}$*

Plasma membrane vesicles exhibit peaks at 1228 and 1267 $cm^{-1}$ (Fig. 3) and a shoulder at 1240 $cm^{-1}$, whereas endoplasmic reticulum has a single peak at 1270 $cm^{-1}$. $\alpha$-Helical homopolypeptides do not reveal strong bands in this region and unordered polypeptides yield rather diffuse Amide III scattering [13]. In contrast, most $\beta$-structured polypeptides exhibit multiple sharp Amide III bands, e.g. 1231, 1276 and 1291 $cm^{-1}$ for poly-L-valine [12], 1231, 1250 and 1268 $cm^{-1}$ for poly-L-alanine [12], 1234, 1252, and 1296 $cm^{-1}$ for $\beta$-pentaglycine [12] and 1220, 1234 and 1295 $cm^{-1}$ for polyglycine I. $\beta$-poly-L-serine [12] and $\beta$-poly-L-lysine exhibit single Amide III bands at 1234 [12] and 1240 $cm^{-1}$ [13].

The data on homopolypeptides indicate that Amide III peaks in the 1220–1240 $cm^{-1}$ region are diagnostic of the $\beta$-conformation. We, therefore, conclude that

the 1228 $cm^{-1}$ band of plasma membranes (and possibly the 1240 $cm^{-1}$ shoulder) arises from $\beta$-structured peptide. This contention is consistent with the infrared and Raman spectra in the Amide I region. In accordance with the Amide I spectra, the Amide III spectrum of endoplasmic reticulum suggests a lack of $\beta$-structure but firm conclusions are difficult due to background luminescence.

*1300–1500 $cm^{-1}$ region*

We observe peaks at 1300, 1340, 1375, 1432, 1440 and 1460 $cm^{-1}$ with plasma membrane and 1340, 1370, 1450, and 1470 $cm^{-1}$ with endoplasmic reticulum (Fig 3; Table I). Studies on various soluble proteins have assigned the bands between 1300 and 1400 $cm^{-1}$ to C-H deformation vibrations and certain ring frequencies of aromatic amino acids [19]. The bands between 1430 and 1470 $cm^{-1}$ arise from the $CH_2$ and $CH_3$ deformation modes of both lipid and protein.

*1000–1200 $cm^{-1}$ region*

The region (Fig. 3; Table I) contains multiple scattering bands arising from C-C, C-N and phosphate stretching vibrations, as well as from tryptophan ring vibrations (1003 $cm^{-1}$, 1015 $cm^{-1}$). The bands at near 1060, 1080 and 1130 $cm^{-1}$ can be ascribed to C-C stretching vibrations of lipid acyl chains. The C-N stretching yield only weak bands in this region. The weak band at 1100 $cm^{-1}$ is due to phosphate.

The 1085 $cm^{-1}$: 1130 $cm^{-1}$ intensity ratio has been used as an index of acyl chain mobility because it decreases in model lipid systems as chain motion increases [20, 21]. The intensity ratio 1085 $cm^{-1}$ : 1130 $cm^{-1}$ of plasma membrane is 0.8 whereas that of endoplasmic reticulum is 1.2. This suggests that the fatty acid chains of endoplasmic reticulum are less mobile than those of plasma membrane. This conclusion fits our evaluation of the 2890 $cm^{-1}$ : 2850 $cm^{-1}$ intensity ratio and with results using the liposome-melittin system. Liposomes of dipalmitoyl lecithin and dipalmitoyl phosphatidylethanolamine yield 1085 $cm^{-1}$ : 1130 $cm^{-1}$ intensity ratios of 2.0 and 0.8 respectively. Binding of melittin increases the ratios to 2.6 and 1.4, respectively, consistent with the known acyl chain immobilization produced by this polypeptide.

*Conjugated double bonds*

Endoplasmic reticulum membranes exhibit prominent peaks at 1528 and 1155 $cm^{-1}$. Both are lacking in plasma membrane, although this does show a shoulder near 1155 $cm^{-1}$. Both bands are less prominent when the samples are excited at 514.5 nm rather than at 488.0 nm. We have observed a strong band at 1530 $cm^{-1}$ in erythrocyte ghosts [6] and have assigned this to resonance-enhanced C=C stretching vibrations of conjugated polyenes, probably carotenoids. The =C–C= stretching vibrations of conjugated systems yield a strong band at 1165 $cm^{-1}$ in free carotenoids and 1170 $cm^{-1}$ in ghosts. In $\beta$-carotene and in ghosts the bands near 1530 and 1170 $cm^{-1}$ are of approximately equivalent intensity, but in rhodopsin [22] or bacteriorhodopsin [23] the band near 1170 $cm^{-1}$ is decreased in relative intensity as is the cases in endoplasmic reticulum.

As documented in refs 3 and 4, the plasma membranes and endoplasmic reticulum differ markedly in protein and lipid composition. The lack of carotenoid adds to these differences but its significance is obscure at present.

*Ring vibrations*

Aromatic ring vibrations are observed at 860, 1003, 1015, 1340 and 1610 $cm^{-1}$. The 860 $cm^{-1}$ is a characteristic of the *p*-hydroxyphenyl ring of tyrosine: the strong band at 1003 $cm^{-1}$ arises from monosubstituted benzenes (e.g. phenylalanine). The 1015, 1340 and 1610 $cm^{-1}$ bands are assigned to the indole rings of tryptophan (Fig. 3; Table I).

*Thermotropism*

We have already shown that the 2890 $cm^{-1}$ : 2850 $cm^{-1}$ intensity ratio can serve as a measure of lipid acyl chain mobility. We have accordingly evaluated this ratio in liposomes and plasma membranes as a function of temperature. In this, we did not use peak intensities but, for liposomes, the integrated scattering between the minima (Fig. 1) at 2860 and 2900 $cm^{-1}$ (for the 2890 $cm^{-1}$ peak) versus the integrated scattering between the minima at 2830 and 2860 $cm^{-1}$ (for the 2850 $cm^{-1}$ peak).

For plasma membranes, we integrated between 2830–2860 and 2875–2895 $cm^{-1}$: this was to avoid interference due to the protein band near 2910 $cm^{-1}$. Our reasons for the integration approach were as follows.

(a) The important factors are the entire populations of bonds giving rise to a particular vibrational mode. Such a population gives rise to scattering over a range of frequencies, not only at the peak frequency.

(b) Varying chain interactions can affect the width of C-H stretching bands. Peak intensity of broad bands cannot be evaluated precisely, whereas the scattering integrated between two frequencies can be very accurate.

In our integration program, the photon counting rates at 2830 and 2860 $cm^{-1}$ (2875 $cm^{-1}$ for plasma membrane) are used to establish the background for the intervals at 2830, 2860 and 2870 $cm^{-1}$, respectively. These two background values are then subtracted from their respective total values to yield the relevant net integrals.

The plot of the integral ratio against temperature (Fig. 2) for egg lecithin liposomes shows a gradual decrease with increasing temperature below 18 °C followed by a sharp drop centered at 20 °C. This discontinuity does not represent the gel to liquid-crystal transition of the phosphatide acyl chains, which occurs at approx. −5 °C (ref. 24 and Verma, S.P. and Wallach, D.F.H., to be published), but may be due to a segregation process.

Egg lecithin/cholesterol liposomes (1 : 1 molar ratio) also show a discontinuity in the plot of the 2890 $cm^{-1}$ : 2850 $cm^{-1}$ scattering ratio vs temperature (Fig. 2). However, this transition now occurs over the whole temperature range studied and is centered at approx. 22 °C.

Lippert and Peticolas [20] have evaluated the gel to liquid-crystal transition of dipalmitoyl lecithin using the 1089 $cm^{-1}$ : 1128 $cm^{-1}$ intensity ratio. They observe a sharp discontinuity at 38 °C, near the known transition temperature, 41 °C, and attribute their low temperature to localized heating. They also found that cholesterol does not abolish transition but broadens it and shifts it to higher temperatures.

Observations on saturated systems [20, 25] show that cholesterol fluidizes the acyl chains below gel to liquid-crystal transition temperature and immobilizes them above the transition temperature. However, our results on egg lecithin/cholesterol

liposomes (containing unsaturated acyl chains) suggest that cholesterol restricts chain mobility both above and below the 20 °C transition, consistent with the suggestion that this transition may represent a segregation process.

A plot of the 2890 $cm^{-1}$ : 2850 $cm^{-1}$ intensity ratio of plasma membrane vesicles versus temperature also shows a striking discontinuity centered at approx. 23 °C. The transition, although less broad than that of cholesterol/lecithin liposomes, still suggests a lesser degree of cooperativity than is observed in lecithin liposomes. Because of interference by protein bands, the amplitudes of the transition in plasma membrane cannot be compared with that in liposomes (Fig. 2). It may represent a phase transition or a segregation phenomenon.

## GENERAL DISCUSSION

We have already commented on various specifics of our Raman spectra and will now discuss their possible relevance to thymocyte membrane structure and function.

First, the Raman spectra indicate the presence of $\beta$-structured polypeptide in plasma membranes of rabbit thymocytes and infrared studies support this observation. In this structural feature, the thymocyte membranes resemble the plasma membranes of rat adipocytes [26]. The possible relevance of $\beta$-structured polypeptide to the similar membrane transport properties and insulin responses of the two cell types [27] remains to be explored.

Second, our Raman data demonstrate a thermotropic phase transition of plasma membrane lipids. If one corrects for the 2–3 °C local heating due to the laser beam, one arrives at a transition temperature of approx. 21 °C, which corresponds closely to that observed by freeze-fracture electron microscopy in the nuclear membranes of lymphoid cells [1]. We must now seek for an explanation of the fact that the nuclear membranes of thymocytes show reversible segregation of membrane proteins below 22 °C, whereas this is not observed in plasma membranes, even after prolonged equilibration at 4 °C [1].

We do not believe that the high cholesterol : phospholipid ratio (approx. 50 mol. %) [2]) of the plasma membranes is an adequate explanation.

Our present data, together with those of Lippert and Peticolas [20] clearly show that cholesterol does not abolish lipid transitions. Moreover, our spectra indicate that the transition in the plasma membranes is much sharper than that of the cholesterol : phospholipid liposomes despite the equivalent sterol : phospholipid ratios of the two systems. If the breadth of the transition is a clue to its "cooperativity" [20] the transition in the membranes is much more cooperative than expected on the basis of cholesterol content. This could come about if the lipids participating in the transition have a lower cholesterol : phospholipid ratio than the total membrane, i.e. with a non-uniform cholesterol distribution.

Since the cholesterol content of the plasma membranes cannot explain the lack of visible protein-lipid segregation, we reason, as before [1], that those proteins represented by the intramembranous particles in the plasma membranes of intact thymocytes cannot undergo unrestricted motion within the membrane cores. The restraining element could be membrane protein or membrane-associated cytoplasmic protein, e.g. microfilaments. It is also conceivable that interactions between phos-

pholipids that are tightly associated with membrane proteins prevent thermotropic lipid-protein segregation.

ACKNOWLEDGMENTS

Supported by awards Nos CA 12178, CB-43922 and CA 13061 from the United States Public Health Service, CB 32123 from the National Science Foundation, PRA-78 from the American Cancer Society (D.F.H.W.) and a grant from the Max-Planck Gesellschaft zur Förderung der Wissenschaften (R.S.-U.).

REFERENCES

1 Wunderlich, F., Batz, W., Speth, V. and Wallach, D. F. H. (1974) Biochim. Biophys. Acta 373, 34–43
2 Schmidt-Ullrich, R., Ferber, E., Knüfermann, H., Fischer, H. and Wallach, D. F. H. (1974) Biochim. Biophys. Acta 332, 175–191
3 Schmidt-Ullrich, R., Wallach, D. F. H. and Ferber, E. (1974) Biochim. Biophys. Acta 356, 288–299
4 Schmidt-Ullrich, R., Wallach, D. F. H. and Hendricks, J. (1975) Biochim. Biophys. Acta 382, 295–310
5 Wallach, D. F. H. and Winzler, R. J. (1974) in Evolving Strategies and Tactics in Membrane Research, Springer-Verlag, New York
6 Wallach, D. F. H. and Verma, S. P. (1975) Biochim. Biophys. Acta 382, 542–551
7 Wallach, D. F. H., Verma, S. P., Weidekamm, E. and Bieri, V. (1974) Biochim. Biophys. Acta 356, 68–81
8 Graham, J. M. and Wallach, D. F. H. (1971) Biochim. Biophys. Acta 241, 180–194
9 Miller, F. A. and Harvey, B. M. (1970) Appl. Spectrosc. 2, 291–292
10 Brown, K. G., Peticolas, W. L. and Brown, E. (1973) Biochem. Biophys. Res. Commun. 54, 358–364
11 Larsson, K. (1973) Chem. Phys. Lipids 10, 165–176
12 Koenig, J. L. (1972) J. Polymer Sci., Part D, 59–177
13 Yu, T., Lippert, J. L. and Peticolas, W. L. (1973) Biopolymers 12, 2161–2176
14 Dollish, F. R., Fateley, W. G. and Bentley, F. F. (1974) in Characteristic Raman Frequencies of Organic Compounds, John Wiley, New York
15 Verma, S. P., Wallach, D. F. H. and Smith, I. C. P. (1974) Biochim. Biophys. Acta 345, 129–140
16 Fanconi, B., Small, E. and Peticolas, W. L. (1971) Biopolymers 10, 1277–1298
17 Koenig, J. L. and Sutton, P. (1971) Biopolymers 10, 89–106
18 Wallach, D. F. H., Graham, J. M. and Oseroff, A. R. (1970) FEBS Lett. 7, 330–334
19 Bellocq, A. M., Lord, R. C. and Mendelsohn, R. (1972) Biochim. Biophys. Acta 257, 280–287
20 Lippert, J. L. and Peticolas, W. L. (1971) Proc. Natl. Acad. Sci. U.S. 68, 1572–1576
21 Mendelsohn, R. (1972) Biochim. Biophys. Acta 290, 15–21
22 Oseroff, A. R. and Callender, R. H. (1974) Biochemistry 13, 4243–4248
23 Mendelsohn, R., Verma, A. L., Bernstein, H. J. and Kates, M. (1974) Can. J. Biochem. 52, 774–781
24 Chapman, D. (1973) in Biological Membranes (Chapman, D. and Wallach, D. F. H., eds), Vol. II, pp. 91–144, Academic Press, London
25 Ladbrooke, B. D., Williams, R. M. and Chapman, D. (1968) Biochem. Biophys. Acta 150, 333–340
26 Avruch, J. and Wallach, D. F. H. (1971) Biochim. Biophys. Acta 241, 249–253
27 Kwock, L. and Wallach, D. F. H. (1974) Biochim. Biophys. Acta 352, 135–145